GIS-based assessment of groundwater vulnerability using DRASTIC: A case study of Ejisu Municipal, Juaben Municipal, and Kwabre East Municipal.

Author: Patrick Azong. **Email:** pazong98@gmail.com

Abstract

Due to the paucity of surface freshwater and its risk of heavy contamination as a result of industrial and domestic activities, people rely mostly on groundwater for survival. Groundwater is very essential because people depend heavily on it for various activities like drinking, cooking, and other activities. In this era of climate change where rainfall patterns have changed greatly and various places experience droughts, groundwater is the sure source of water for human survival. This study used the DRASTIC method to assess groundwater vulnerability potential to contamination in selected municipalities in the Ashanti Region. This method employs hydrogeological and anthropogenic factors to determine the vulnerability potential of groundwater to contamination. The method was used in collaboration with the Inverse Distance Weighted (IDW) interpolation method to give a vivid understanding of groundwater vulnerability. Both raster and vector data sets were used in the QGIS and SPAW environments to arrive at the results of the study. The study has shown that most parts of the area are at low risk of groundwater vulnerability potential to contamination. This is because the parameters with a high impact on the groundwater vulnerability based on their weights and rates show low vulnerability potential to pollution.

Keywords: Groundwater, DRASTIC, Groundwater contamination, Multi-criteria Analysis.

1. Introduction

Water is essential for human life and constitutes about 75% of the Earth's surface (Dumedah et al., 2021). We essentially depend on water for most of our domestic, agricultural, and industrial activities. It is estimated that 2.5% of the 75% water content of the Earth's surface is freshwater (Dumedah et al., 2021). The inadequate availability of surface freshwater coupled with improper planning and industrial activities that pollute water bodies often leads to water insecurity (Kale & Pawar, 2017), making arid regions suffer high risks (Li et al., 2021). Human activities such as illegal mining, and the use of chemicals in farming and fishing have greatly suppressed the quality of surface water (Assefa & Dinka, 2023; Dumedah et al., 2021). Due to the limited availability of surface fresh water, about 1.5 billion people worldwide rely majorly on groundwater as their major source of fresh water (Adimalla & Li, 2019; Barbulescu, 2020; Bera et al., 2021; He et al., 2015).

Groundwater is a vital source of freshwater on earth and comprises nearly half the water used domestically, and for agricultural activities (Patel et al., 2022). For this study, groundwater vulnerability is the propensity of the groundwater system to get contaminated with pollutants, especially from the activities of man that percolate into it (Bărbulescu & Barbeş, 2020; Ikenna & Chibuike, 2021). When the groundwater system is contaminated, it causes serious devastating effects on the lives that depend on it for survival. For instance, in the 1850s, contamination of water led to the breakout of cholera in Broad Street, London (Brody et al., 2000). This disease outbreak claimed many lives until John Snow came up to the scene by using mapping techniques to trace the cause to a contaminated water pump (Johnson, 2007). This is an instance of how the contamination of water especially the groundwater system can cause devastating effects to humanity. To spatially target the risk levels and contamination of groundwater to restore its quality, it becomes difficult and requires a multi-criteria approach to work it out (Dumedah et al., 2021; Falkenmark, 2003). Many factors or variables work together to determine groundwater vulnerability levels hence the need to employ methods that holistically use hydrogeological parameters to determine areas at risk of groundwater contamination. Maps can be constructed to show how the factors used to assess vulnerability impact the risk of groundwater contamination to help guide decision-making (Barbulescu, 2020; Bera et al., 2021; Vrba, 2016).

Vulnerability assessment is a crucial step in identifying areas where groundwater is most susceptible to contamination, allowing for targeted measures to prevent pollution and ensure the

long-term sustainability of this vital resource (Vrba, 2016). To manage and protect groundwater resources effectively, it is essential to understand their extent of vulnerability to contamination (Foster, 2019). While several assessment tools have been used for groundwater vulnerability assessment including the Heavy Metal Pollution Index (HPI) (Boateng et al., 2019), Contamination and Pollution Load Factors (Appiah-Adjei et al., 2016), Weighted Quality Index (WQI) (Amiri et al., 2014), the DRASTIC index has been a popular and effective method used due to its holistic integration of several factors and ability to give a comprehensive understanding of groundwater quality (Aboagye & Zume, 2018). DRASTIC is an acronym that stands for depth to groundwater, net recharge, aquifer media, soil media, topography (slope), impact of the vadose zone, and hydraulic conductivity (Aller et al., 1987). While most of these methods for assessing groundwater vulnerability to pollution have been extensively applied in Ghana, these methods are either based on specific pollutants or current water quality instead of vulnerability. The DRASTIC model therefore stands out as it uses hydrogeological factors to comprehensively assess groundwater vulnerability and also serves as a predictive tool to predict areas at risk of groundwater contamination. This means the model considers both natural (slope and soil type) and human factors (land use) to give a holistic understanding of groundwater vulnerability.

This study filled this methodological gap of groundwater vulnerability assessment by utilizing the DRASTIC model together with the Inverse Distance Weight (IDW) interpolation method to assess groundwater vulnerability to pollution in three municipalities of the Ashanti Region, Ghana. The study explored the seven DRASTIC parameters by adopting a multi-criteria approach.

2. Material and Methods

2.1 Study Area

This study was conducted in three (3) major municipalities (the Ejisu municipality, Juaben municipality, and Kwabre East municipality) in the Ashanti Region of Ghana where people rely mostly on groundwater for survival. The information in Figure 1 shows these three municipalities merged together.

The Ejisu Municipality an area of about 1,782.2km² and located within longitudes 1°5W and 1°39’ W, and latitudes 7°9’ N and 7°36’N (Ghana Districts, n.d.). According to the 2021 population and housing census report, the municipality has a population of 180,723 comprising

87,836 males and 92,887 females. The municipality is bounded to the northeast and northwest by Sekyere East District and Kwabre East Municipal respectively, to the south by Bosomtwe District and Asante Akim South Municipal, to the east is the Asante Akim North Municipal and to the west is the Kumasi Metropolitan (Ghana Districts, n.d.). It has mean monthly temperatures of about 20 °C in August and 32 °C in March and experiences its rainfall peak in August (T. Boateng et al., 2016). The municipality relies heavily on groundwater for domestic and industrial activities.

The Juaben Municipality also has a total area of 365 sq. km and lies within latitudes 1° 15’ N and 1° 45’ N, and longitudes 6° 15’ W and 7° 00’ W. The municipality is boarded to the north-east by the Sekyere East and Kwabre East Municipal on the north-west, Ejisu Municipal to the west, Bosomtwe District on the south-west, Asante Akim Central Municipal on the east, and the Kumasi Metropolitan Assembly on the north (Ghana Districts, n.d.). The municipality has a population of 63,929 with 31,203 males and 32,726 females. This region has a tropical climate with high temperatures and high humidity throughout the year.

The Kwabre East Municipality has a total land area of about 148 square kilometers and lies within latitudes 6° 45’N and 6° 50’N, and longitudes 1° 30’W to 1° 35’W. The municipality is bordered by the Sekyere South district to the north, Kumasi Metropolitan Assembly to the south, Ejisu Municipal to the southeast, Atwima Nwabiagya Municipal to the west, and Offinso Municipal to the northwest. The population in 2020 is 296,814 with 143,684 males and 153,130 females. The vegetation of Kwabre East Municipal is dense forest and grassland.

Figure 1. Ejisu, Juaben and Kwabre East Municipalities merged together

2.2 Data Sources

Two major categories of data sets were used in this study, including vector and raster data. The vector data is in the shapefile (.shp) format and they include towns, roads, and polygon data of the districts under study. The raster data was in the Georeferenced Tagged Image File Format (GeoTIFF). The individual raster data sets include, Digital Elevation Model (DEM), Soil (comprising sand, silt, and clay), evapotranspiration (from 2003 to 2019), rainfall/precipitation (covering the 12 months), and land use. The DEM data was obtained as Shuttle Radar Topography Mission 1 Arc-Second Global (SRTM) data from the American Geological Survey Department's (USGS) website with a 30m resolution. The evapotranspiration data was acquired from the Famine Early Warning Systems Network (FEWS-NET) website with a 1.1km per grid resolution. Evapotranspiration (ET) combines transpiration from vegetation and evaporation from the soil and surface water bodies. Actual ET (ETa) is produced using the operational Simplified Surface Energy Balance (SSEBop) model (Senay et al., 2012) from 2003 to 2019. It combines ET fractions generated from remotely sensed MODIS thermal imagery with reference ET using a thermal index approach. The Rainfall data was downloaded with 30 seconds (~1 km^2) spatial resolution as a GeoTIFF. It was obtained from the WorldClim website. The soil data was also downloaded from the SoilGrid website with a 250m resolution. The depth of each soil type ranges from 0cm to 200cm. This was divided in six different sub depths including 0-5cm, 5-15cm, 15-30cm, 30-60cm, 60-100cm, and 100-200cm. All these divisions were classified into zones with zone one representing 0-5cm, zone two representing 5- 15cm, zone three representing 15-30cm, zone four representing 30-60cm, zone five representing 60-100cm, and zone six represents 100-200cm. In addition, the land use data was downloaded from the United States Geological Survey Earth Resources Observation & Science (EROS) Center website. The different vector data sets were obtained from DIVA-GIS and Natural Earth.

2.3 Data Preparation and preprocessing.

Each of the individual data sets in the vector and raster categories were reprojected from the Geographic Coordinate System, which is the World Geodetic System 1984 (WGS 84) in angular units to the projected coordinate reference system according to the Universal Transverse Mercator (UTM) projection. WGS84 UTM zone 30N was used since the Ashanti region of Ghana falls within that zone of the UTM zone classifications. The reprojection was necessary as I needed to

do some calculations or data manipulation activities and hence the angular units are not preferable for such tasks. The raster data was resampled to ensure that the spatial resolutions of the different data sets match since the study involves a multi-criteria analysis. The fine raster data sets were resampled to change their pixel size to match those of the coarse raster data sets. Most of the data was downloaded in raster Tiles so I merged (mosaicked) the data sets and extracted (clipped raster by masked layer) the area of interest for this study.

2.4 Study Approach

The analysis of the above-mentioned data involved a multi-criteria approach. The approach used was the DRASTIC model which was first used by the United States Environmental Protection Agency (EPA) to assess groundwater vulnerability to contamination. The software used in this study are Quantum Geographic Information System (QGIS), Soil Plant Air Water (SPAW), and System for Automated Geoscientific Analyses (SAGA) which is embedded in the earlier versions of QGIS.

The final DRASTIC index uses ratings and weightings assigned to the seven parameters of the model to obtain the final DRASTIC index. Each parameter is subdivided into significant media and assigned a weight from 1 to 5 based on their relative importance and also assigned ratings from 1 to 10 according to their relative impact on pollution potential. The DRASTIC Index (DI) is then calculated by applying a linear combination of the parameters or factors as $DRASTIC\ Index\ (DI) = DrDw + RrRw + ArAw + SrSw + TrTw + Ir\ Iw + CrCw$ (Patel et al., 2022; Shakoor et al., 2020). The subscripts r and w are the ratings and weightings respectively (Ikenna & Chibuike, 2021). The weight of each variable is multiplied by its rating for all the parameters and subsequently added to obtain the DRASTIC index. The model used the traditional weights assigned by Aller et al., (1987). The information in Table 1 below represents the weights of each parameter (variable) in the model.

Table 1. DRASTIC Parameter Weightings

VARIABLES	WEIGHT
Depth to Water (D)	5
Net Recharge (R)	4
Aquifer Media (A)	3

Soil Media (S)	2
Topography/Slope (T)	1
Impact of Vadose Zone (I)	5
Hydraulic Conductivity (C)	3

3. Results and Discussion

3.1 Depth to Groundwater table (D)

This parameter of the model represents the depth from the ground surface to the underground water (Ikenna & Chibuike, 2021). A deeper depth to the groundwater table means a lesser chance of contaminants infiltrating into the groundwater system and a shallower depth to the groundwater table means a higher possibility of pollutants getting to the water table and hence high potential underground water contamination (Assefa & Dinka, 2023). This parameter was derived from static water or well level data in the area of interest by measuring the depths of wells in and around the Ashanti Region in meters. However, it can also be one reported by research projects or the Hydrological Service Department. The average figure was then subtracted from the DEM data to obtain the Depth to the groundwater table. The results in Figure 2from this analysis show that the D values range from 100m to 600 meters. These values were then reclassified into 5 classes to aid the interpretation of the results. The information in Figure 2 shows the southeastern part of the area has very high groundwater vulnerability potential while the extreme southwest has very low groundwater vulnerability potential. However, a major part of the area (about 70%) covering the central part has high groundwater vulnerability potential. Based on this parameter, the area is likely to have its groundwater contaminated due to the generally low depths obtained.

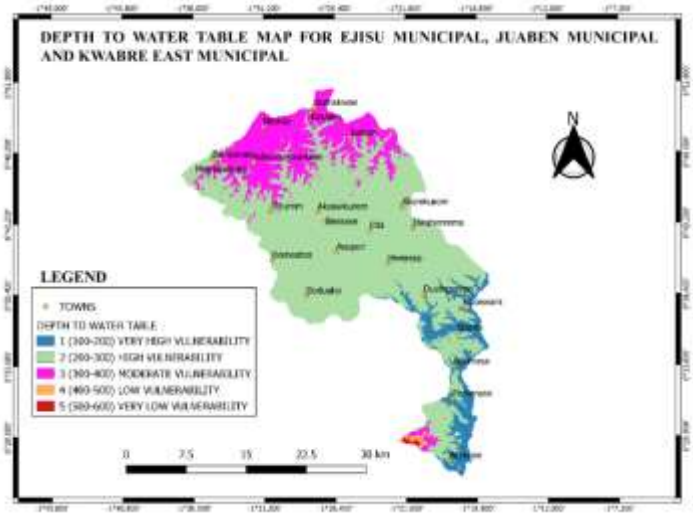

Figure 2. Depth to the groundwater table

3.2 Net recharge (R)

This variable refers to the net amount of water that penetrates the surface to the ground and reaches the water table (Assefa & Dinka, 2023; Ikenna & Chibuike, 2021). Simply, it is the annual total amount of water that infiltrates into the aquifer. Most of the water gets intercepted by elements like trees, buildings, and vegetation. For this reason, the precipitation data must be corrected. Net recharge is a significant medium through which ground contaminants are carried because pollutants percolate vertically into the water table. This parameter was derived using the formula, $NR = P - (ETa + Q)$ where NR = Net Recharge, P = Precipitation (mm/yr.), Eta = Actual Evapotranspiration, and Q = Runoff. The runoff (Q) was determined using the formula, Q = P * k, where P is annual rainfall within the area of interest, and k represents the runoff coefficient. The hydrologic soil groups, the land cover types, the residential density, and the slope (in percentage) of the area are factors used to determine the runoff coefficient (k). The runoff coefficient is a dimensionless coefficient relating the amount of runoff to the amount of precipitation received. It has large values for areas with low infiltration and high runoff (for instance, steep gradients), and low values for permeable, well-vegetated areas (for instance forests or flat lands). The residential density and land cover types can be obtained through digitizing high-resolution satellite imagery for characterization. However, for this study, land cover raster data was used. The k was determined by generating random sample locations in the area of interest to obtain the known values of the slope (calculated in percentages), the land cover types, and the hydrologic soil groups. This means that in the attribute table of the random point locations obtained, fields were created

for the slope, land cover type, and hydrologic soil groups and the sample raster values tool in QGIS was used to get their known raster values. The raster values for the land cover data were used in collaboration with the MODIS land cover lookup table to get the land cover types. The lookup table for the land cover types can be found in the user guide documentation on this website. The hydrologic soil groups were obtained by using the soil textures obtained from the soil media to determine their permeability codes which were then used to get their hydrologic soil groups. Information about the soil permeability codes can be obtained here. A fourth field was created on the attribute table of the sample point locations generated to contain the runoff coefficient values which were determined by comparing the known values of the 3 initial fields (slope, land cover, and hydrologic soil groups) to get their associated runoff values at the sample locations. The comparison was done with insights from the runoff coefficient lookup table on the Bright Hub Engineering website. Inverse Distance Weight (IDW) interpolation was undertaken using the runoff coefficient values to get the runoff coefficient of the entire area as a raster data set. After that, the raster calculator was used to do the calculations to get the Q and ultimately the NR. The results from this analysis show that the net recharge values range from -500 to 1100mm. The higher (larger) the values obtained, the larger the amount of water the ground receives and vice versa. The majority of the areas have moderate net recharge while very few areas have very high net recharge and very low net recharge. This information is shown in Figure 3 below.

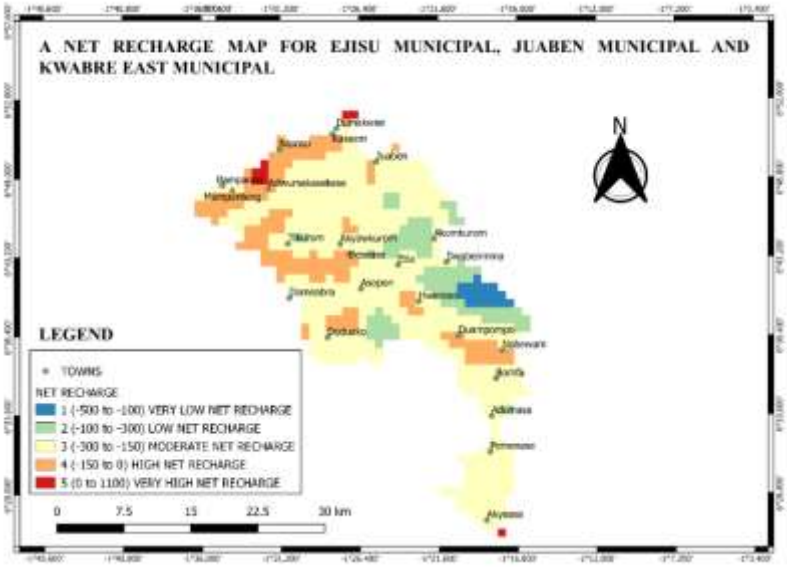

Figure 3. Net Recharge of the Area.

3.3 Aquifer Media (A)

This is a zone with saturated soil properties that influence the process of pollutant attenuation and lies below the vadose zone. The porous spaces and fractures where water is held, make up this media. The attenuation capacity of the aquifer media depends on the size and amount of its grains – the finer the grains, the higher the attenuation capacity (Assefa & Dinka, 2023; Bera et al., 2021; Samake et al., 2011). This parameter was derived by determining the soil texture classes of the zone six of each of the three different soil groups. The soil texture class values were determined using the SAGA soil texture classification in QGIS 3.10. These values were then compared with the SAGA soil texture class lookup table on their website. The results in Figure 4 show that sandy clay loam is the major soil type in the area with patches of silt, loam, loamy sand, and silty clay loam. This information is presented in

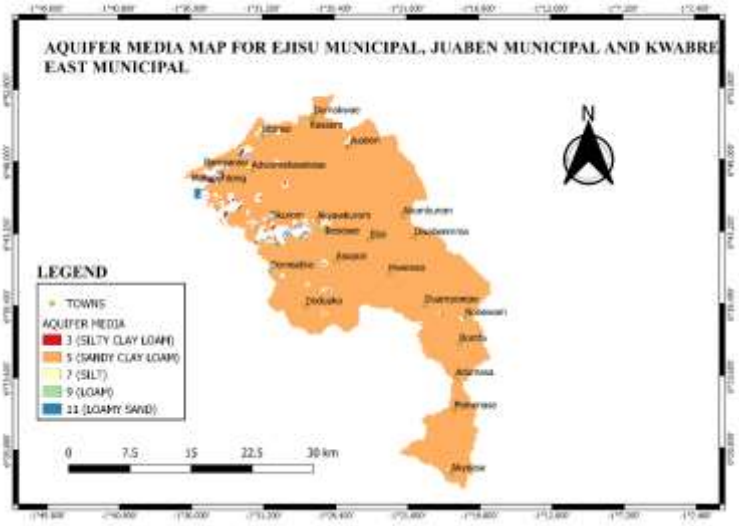

Figure 4. Aquifer media of the area.

3.4 Soil Media (S)

Soil media is the uppermost and mostly weathered part of the unsaturated zone that influences the amount of recharge infiltrating vertically underground (Patel et al., 2022). This allows water and contaminants to be transported to the aquifer. This zone lies directly above the vadose zone. It provides the initial defense to pollutant infiltration (Shakoor et al., 2020). Different characteristics such as texture, structure and compaction significantly control the infiltration rate of surface water to the underground water system. This parameter was derived by determining the average soil proportions for all the soil texture groups (sand, silt, and clay) categorized in zones,

using the formula (*zone one+zone two*)/2 with the help of the raster calculator. The average of zone 1 and 2 of each of the three different soils was used in the SAGA soil texture classification to determine their soil texture values. These values were then compared with the SAGA soil texture class lookup table on their website. The results found were not different from those in the aquifer media.

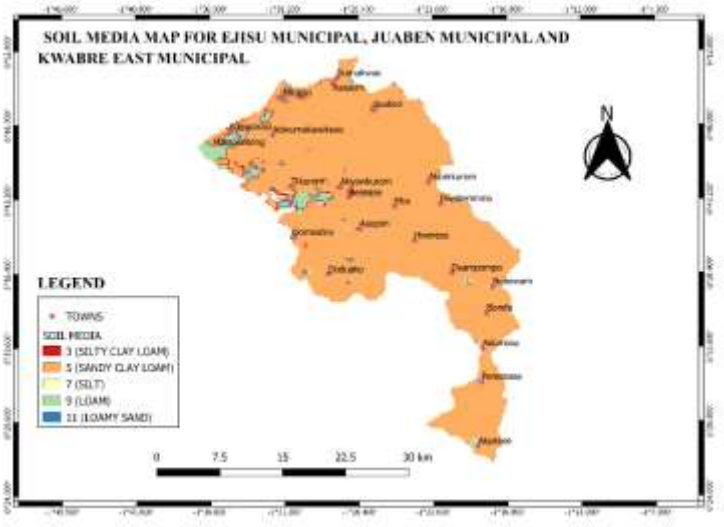

Figure 5. Soil Media of the Area

3.5 Topography (T)

The topography in this model represents the slope of the terrain of the area (Patel et al., 2022). The rate of flow at the surface that influences biodegradation and attenuation is shown by this factor. The slope determines whether an area will experience higher surface runoff or infiltration which allows surface contaminant percolation to the water table. Water that is retained in areas with lower slopes increases the rate of infiltration and, subsequently has a greater possibility for transporting contaminants. This means that gentle slopes encourage higher infiltration of water and contaminants while steep slopes encourage high runoff and low infiltration of water and contaminants. The slope was calculated using the Geographic Data Abstraction Library (GDAL) in QGIS. The information in Figure 6 shows that majority of the area shows low/gentle slope with few areas especially the south western part showing very steep slopes. This means water is like to flow in the southern western part while accumulated in the other areas indicated as low/gentle slopes.

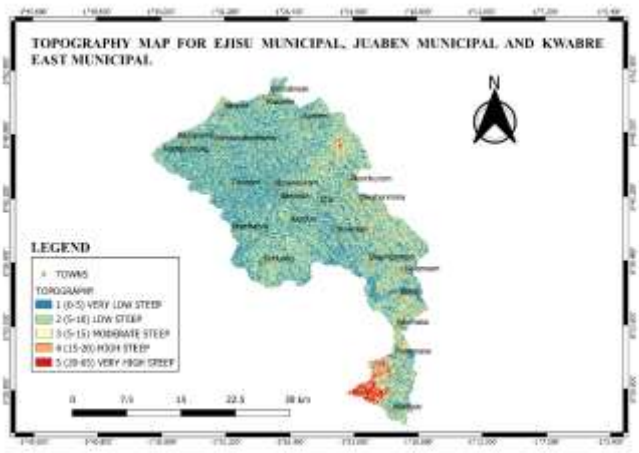

Figure 6. Slope of the Area

3.6 Impact of the Vadose Zone (I)

This is an unsaturated or discontinuous zone lying between the soil media and the aquifer media. Several processes controlling pollution potential occur within this zone which also influences the attenuation and passage of contaminated substances to the aquifer (water table) (Assefa & Dinka, 2023; Patel et al., 2022). This parameter was determined using the expression; (*zone three + zone four + zone five*)/3. This means that the averages of zones 3, 4, and 5 of each of the three soil types (sand, silt, and clay) were determined using the above expression, and the soil texture was calculated in SAGA soil texture classification. The results were then compared with the SAGA soil texture class lookup table to determine the corresponding soil texture classes. The results in Figure 7 show that the dominant soil texture class is sandy clay loam followed by sandy clay and clay loam. The list dominant among them is the silt loam.

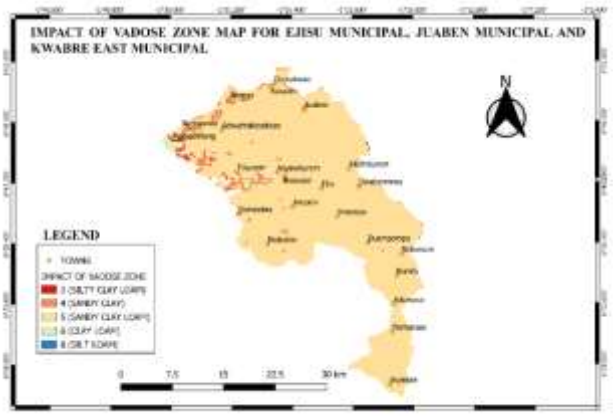

Figure 7. Impact of the Vadose zone

3.7 Hydraulic Conductivity (C)

This represents the ability of the aquifer to transmit water (Assefa & Dinka, 2023). It dictates the rate of flow of contaminant materials within the groundwater system. Higher conductivity means higher infiltration and possibility for contaminants to be carried. To get this parameter, a water budgeting tool for farm fields, ponds and inundated wetlands developed by the United States Department of Agriculture was used. Soil Water Characteristics is a program within the software installation that is used to simulate soil water tension, conductivity and water holding capability based on the soil texture, with adjustments to account for gravel content, compaction, salinity, and organic matter. This software is called SPAW (Soil Plant Air Water). The hydraulic conductivity in this model has to do with the movement of water in the aquifer media hence the saturated hydraulic conductivity values were determined for each of the soil types identified under the aquifer media calculation. The results show that the saturated hydraulic conductivity values range from 0.03in/hr to 4.49in/hr and as stated earlier, high values indicate high hydraulic conductivity and consequently high pollutants transmission. The information in Figure 8 below demonstrates that loamy sand has the highest saturated hydraulic conductivity (4.49in/hr) while silty clay loam has the lowest saturated hydraulic conductivity values (0.03in/hr). Therefore, this presupposes that the areas covered by loamy sand and loam will likely have high groundwater contamination because the movement of groundwater there is much faster than in areas covered by silty clay loam and sandy clay loam. This shows over 80 percent of the area has very low hydraulic conductivity.

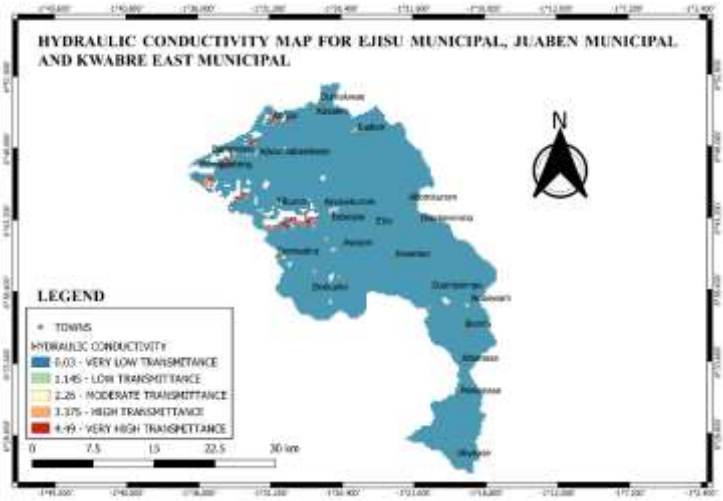

Figure 8. Hydraulic Conductivity

3.8 Final DRASTIC Index

A multi-criteria evaluation was finally undertaken to determine the DRASTIC index after all the individual parameters were obtained. This was determined using the formula, DRASTIC Index = D5D5 + R4R4+ A2A2 + S2S2+ T1T1+I5I5 +C3C3. This was achieved with the help of the raster calculator in QGIS. Each rating was multiplied to its corresponding weighting and the results were summed to get the final DRASTIC index. This index gives a holistic understanding of the groundwater contamination potential of the area by combining the seven hydrogeological parameters calculated. The results show that the eastern part of the area covered by communities such as Akumkurom, and Dwabenmma has low groundwater contamination potential while the northwestern part of the area covered by communities such as Ntonso, Adwumakasekese, and Kasaem have high groundwater contamination potential. This means that government and other agencies should work on treating the groundwater sources of areas identified to have high groundwater vulnerability to contamination on regular basis to help prevent or reduce the health implications associated with contaminated drinking water. If the situation becomes bad, these communities should be relocated to areas where the groundwater is good for consumption and domestic use.

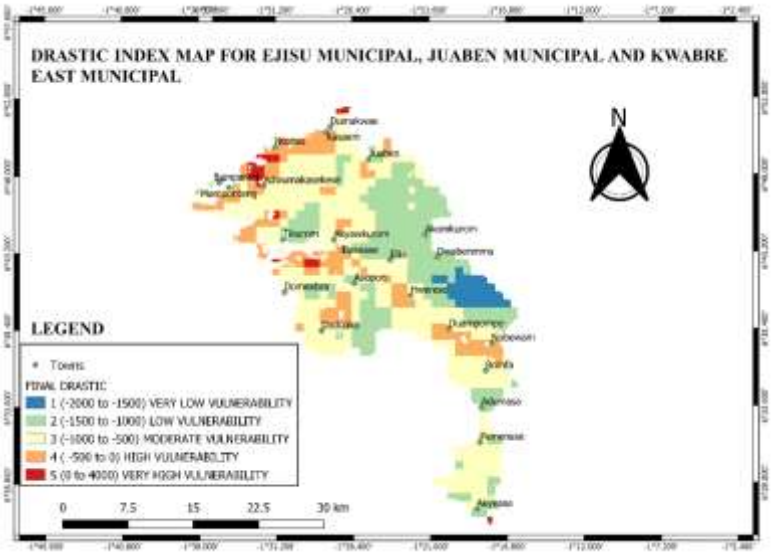

Figure 9. DRASTIC Index

3.9 DRASTIC Automation

Estimating the DRASTIC index involves complex processes and procedures which consumes a lot of time and can often result in making mistakes. To help reduce time and work faster, there are various procedures for work automation. In this study, I have used the Graphical Modeler to demonstrate the complex processes involved in estimating the DRASTIC index, thereby reducing time and minimizing errors in future studies. Models can be built for each task performed in the software to enhance efficiency. The graphical modeler has access to both the field calculator (suitable for manipulating vector attribute data), the raster calculator (suitable for manipulating raster data), and numerous algorithms and inputs hence making it more suitable for automation tasks. The information in Figure 10 is a picture of the model I built with the graphical modeler to help automate similar works in the future and as stated earlier, a model can be built for each task performed in the software (QGIS). This picture might look simple but contains many procedures or steps at the backend.

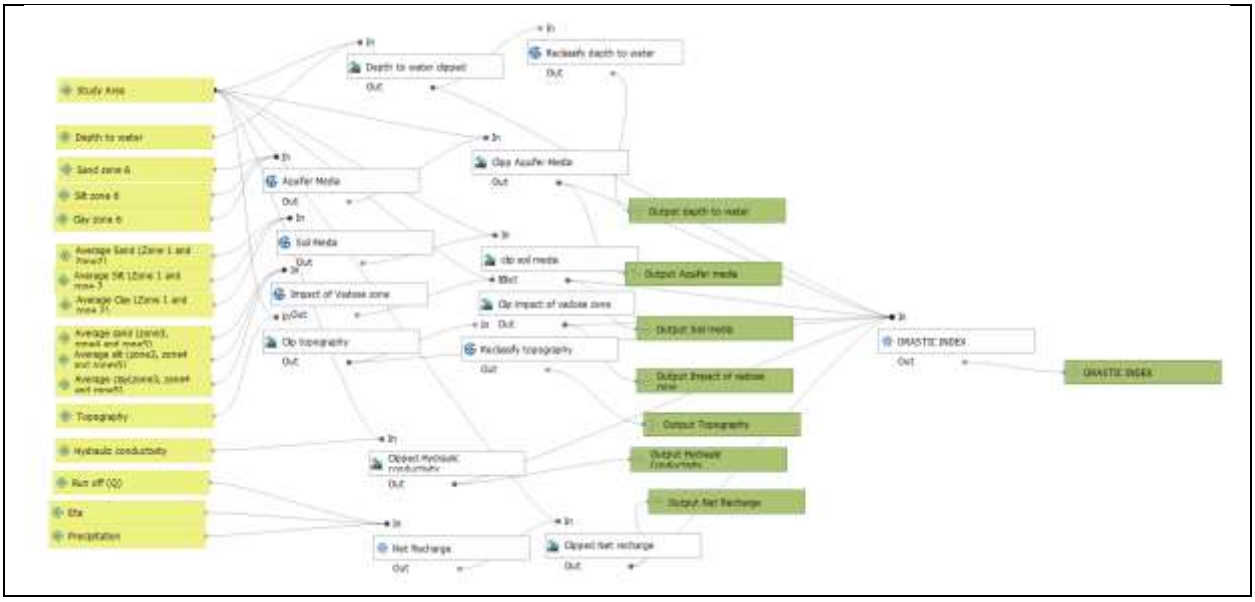

Figure 10. Graphical Modeler.

4. Discussion and Conclusion

Each of the parameters used in this study is essential in deriving the final DRASTIC index but the parameters examined in isolation are not enough to make reliable conclusions on the groundwater vulnerability potential in the area hence the need to combine all of them. This study has found that a major part of the area especially the eastern, central, and southern parts

experiences low groundwater vulnerability. However, the northwestern, and western parts are the areas identified to have high groundwater contamination potential. This high vulnerability potential may be due to the impact of the high-rating net recharge which showed similar results in those areas. The insights from this study is essential for governments and water resource organizations to help plan on how to get potable water for various communities in the area. Also, it will give crucial information to the municipal assemblies in their routines of getting healthy water for the people in the municipalities. These results are consistent with the findings of Assefa & Dinka, (2023) who also found that major parts of the Doornfontein area, near the central business district of Johannesburg has low groundwater vulnerability while a small part has high groundwater vulnerability to pollution. However, the findings of Aboagye & Zume, (2018) shows otherwise. This inconsistency may be because their studies have been conducted in different districts or because their study is conducted in specific water wells and their emphasis were on specific pollutants.

References

Aboagye, D., & Zume, J. (2018). Assessing Groundwater Quality in Peri-urban Localities of Kumasi, Ghana. *African Geographical Review*. https://doi.org/10.1080/19376812.2018.1484781

Adimalla, N., & Li, P. (2019). Occurrence, health risks, and geochemical mechanisms of fluoride and nitrate in groundwater of the rock-dominant semi-arid region, Telangana State, India. *Human and Ecological Risk Assessment: An International Journal*, *25*(1–2), 81–103. https://doi.org/10.1080/10807039.2018.1480353

Aller, L., Bennett, T., Lehr, J., Petty, R., & Hackett, G. (1987). DRASTIC: Standardized system for evaluating groundwater pollution potencial using hydrogeologic settings. *Journal of the Geological Society of India*, *29*.

Amiri, V., Rezaei, M., & Sohrabi, N. (2014). Groundwater quality assessment using entropy weighted water quality index (EWQI) in Lenjanat, Iran. *Environmental Earth Sciences*, *72*(9), 3479–3490. https://doi.org/10.1007/s12665-014-3255-0

Appiah-Adjei, E. K., Appiah, N. F., & Adjei, K. A. (2016). Potential groundwater pollution from improper oil and metal waste disposal in Suame, Ghana. *Journal of Science and Technology (Ghana)*, *36*(3), 20–33.

Assefa, A., & Dinka, M. (2023). Groundwater Vulnerability AssessmentUsing Modified DRASTIC Index, the Caseof Doornfontein Area (Johannesburg). *Polish Journal of Environmental Studies*, *32*(2), 1037–1048. https://doi.org/10.15244/pjoes/154742

Barbulescu, A. (2020). Assessing groundwater vulnerability: DRASTIC and DRASTIC-like methods: a review. *Water*, *12*(5), 1356.

Bărbulescu, A., & Barbeş, L. (2020). Assessing the water quality of the Danube River (at Chiciu, Romania) by statistical methods. *Environmental Earth Sciences*, *79*(6), 122. https://doi.org/10.1007/s12665-020-8872-1

Bera, A., Mukhopadhyay, B. P., Chowdhury, P., Ghosh, A., & Biswas, S. (2021). Groundwater vulnerability assessment using GIS-based DRASTIC model in Nangasai River Basin, India with special emphasis on agricultural contamination. *Ecotoxicology and Environmental Safety*, *214*, 112085. https://doi.org/10.1016/j.ecoenv.2021.112085

Boateng, T. K., Opoku, F., & Akoto, O. (2019). Heavy metal contamination assessment of groundwater quality: A case study of Oti landfill site, Kumasi. *Applied Water Science*, *9*(2), 33. https://doi.org/10.1007/s13201-019-0915-y

Boateng, T., Opoku, F., Acquaah, S., & Akoto, O. (2016). Groundwater quality assessment using statistical approach and water quality index in Ejisu-Juaben Municipality, Ghana. *Environmental Earth Sciences*, *75*. https://doi.org/10.1007/s12665-015-5105-0

Brody, H., Rip, M. R., Vinten-Johansen, P., Paneth, N., & Rachman, S. (2000). Map-making and myth-making in Broad Street: The London cholera epidemic, 1854. *The Lancet*, *356*(9223), 64–68. https://doi.org/10.1016/S0140-6736(00)02442-9

Dumedah, G., Moses, A., & Linda, G. (2021). Spatial targeting of groundwater vulnerability in the Wewe-Oda river watershed in Kumasi, Ghana. *Groundwater for Sustainable Development*, *14*, 100641.

Falkenmark, M. (2003). Freshwater as shared between society and ecosystems: From divided approaches to integrated challenges. *Philosophical Transactions of the Royal Society of London. Series B: Biological Sciences*, *358*(1440), 2037–2049. https://doi.org/10.1098/rstb.2003.1386

Ghana Districts. (n.d.). *Ghana Districts: A repository of all Local Assemblies in Ghana*. Retrieved October 30, 2024, from https://www.ghanadistricts.com/Home/District/18

He, J., Ma, J., Zhao, W., & Sun, S. (2015). Groundwater evolution and recharge determination of the Quaternary aquifer in the Shule River basin, Northwest China. *Hydrogeology Journal*, *23*(8), 1745–1759. https://doi.org/10.1007/s10040-015-1311-9

Ikenna, I., & Chibuike, I. (2021). GIS-based evaluation of shallow aquifer vulnerability to pollution using DRASTIC model: A case study on Abakaliki, southeastern, Nigeria. *Arabian Journal of Geosciences*, *14*. https://doi.org/10.1007/s12517-021-08811-8

Johnson, S. (2007). *The ghost map: The story of London's most terrifying epidemic and how it changed science, cities, and the modern world* (Paperback ed). Riverhead.

Kale, S., & Pawar, N. J. (2017). Fluoride accumulation in groundwater from semi-arid part of Deccan Volcanic Province, India: A cause of urolithiasis outbreak. *Hydrospatial Anal*, *1*, 9–17.

Li, P., Karunanidhi, D., Subramani, T., & Srinivasamoorthy, K. (2021). Sources and Consequences of Groundwater Contamination. *Archives of Environmental Contamination and Toxicology*, *80*(1), 1–10. https://doi.org/10.1007/s00244-020-00805-z

Patel, P., Mehta, D., & Sharma, N. (2022). A review on the application of the DRASTIC method in the assessment of groundwater vulnerability. *Water Supply*, *22*(5), 5190–5205.

Samake, M., Tang, Z., Hlaing, W., Mbue, I. N., Kasereka, K., & Balogun, W. O. (2011). Groundwater vulnerability assessment in shallow aquifer in Linfen Basin, Shanxi Province, China using DRASTIC model. *Journal of Sustainable Development*, *4*(1), 53.

Senay, G. B., Bohms, S., & Verdin, J. P. (2012). *Remote sensing of evapotranspiration for operational drought monitoring using principles of water and energy balance*. https://digitalcommons.unl.edu/usgsstaffpub/979/

Shakoor, A., Khan, Z. M., Farid, H. U., Sultan, M., Ahmad, I., Ahmad, N., Mahmood, M. H., & Ali, M. U. (2020). Delineation of regional groundwater vulnerability using DRASTIC model for agricultural application in Pakistan. *Arabian Journal of Geosciences*, *13*(4), 195. https://doi.org/10.1007/s12517-020-5161-y

Vrba, J. (2016). The role of groundwater governance in emergencies during different phases of natural disasters. *Hydrogeology Journal*, *24*(2), 287.